RSC Advances

PAPER

View Article Online
View Journal | View Issue



Cite this: *RSC Adv.*, 2024, **14**, 1665

# Construction of a conjugated covalent organic framework for iodine capture†

Chao Gao, ‡ Xuhui Guan,‡ Lei Chen, Haoran Hu, Lei Shi, Chong Zhang, Chengguo Sun, Yang Du and Bingcheng Hu *

Radioactive iodine in the nuclear field is considered very dangerous nuclear waste because of its chemical toxicity, high mobility and long radioactive half-life. Herein, a conjugated two-dimensional covalent organic framework, TPB-TMPD-COF, has been designed and synthesized for iodine capture. TPB-TMPD-COF has been well characterized by several techniques and showed long order structure and a large surface area (1090 $m^2\ g^{-1}$). Moreover, TPB-TMPD-COF shows a high iodine capture value at 4.75 g $g^{-1}$ under 350 K and normal pressure conditions, benefitting from the increased density of adsorption sites. By using multiple techniques, the iodine vapor adsorbed into the pores may readily generate the electron transfer species ($I_3^-$ and $I_5^-$) due to the strong interactions between imine groups and iodine molecules, which contributes to the high iodine uptake for TPB-TMPD-COF. Our study will stimulate the design and synthesis of COFs as a solid-phase adsorbent for iodine uptake.

Received 14th November 2023
Accepted 25th December 2023

DOI: 10.1039/d3ra07781k

rsc.li/rsc-advances



## Introduction

Nuclear energy has been widely used in human society, including military, energy, industry, aerospace and other fields, which has a significant impact on energy development.[1] However, with the development of nuclear energy, one of the problems we have to face is the disposal of nuclear waste produced from nuclear fission, which has a great impact on the living environment of human beings. As a volatile side product of nuclear fission reaction, radioactive $^{129}I$ is considered the most dangerous nuclear waste due to the long radioactive half-life (15.7 million years).[2] To date, many efforts have been made to develop new methodologies for removing radioactive $^{129}I$, in which solid-phase adsorption is believed to have considerable prospects.[3] Therefore, the search of novel porous materials for efficient capture and removal of radiological iodine has attracted significant research interest.

Covalent organic frameworks (COFs),[4] as an emerging class of porous crystalline materials, are precisely assembled from organic building blocks into periodic structures. Compared to other porous materials, COFs are connected by chemically stable covalent bonds, rendering them superior thermal and chemical stability. Since they were first reported in 2005 by Yaghi *et al.*,[5] COFs have attracted much attention and have shown great potential in various applications, such as sorption and separation,[6] sensing,[7] energy,[8] catalysis,[9] and so on. Due to their high surface area, low density and regular pore structure, COFs are suitable as a solid-phase adsorbent and have been studied as adsorbent materials for iodine capture.[10–21] For example, Fang *et al.* synthesized tetrathiafulvalene-based COFs and achieved excellent iodine adsorption capacity through the synergistic effect of physical and chemical adsorption.[16] Recently we have also reported a pyrene-based two-dimensional COF (TFPPy-TMPD-COF) with a vapor capacity of 4.8 g $g^{-1}$ due to the combination of chemisorption and physisorption,[19] in which the introduction of 2,3,5,6-tetramethyl-*p*-phenylenediamine (TMPD) was helpful for changing the pore environment to enhance the iodine adsorption capacity of the COF. However, the relatively low density of chemical adsorption sites (*e.g.*, C=N group) in TFPPy-TMPD-COF still restricted its iodine capacity. Therefore, we anticipated that further increasing the density of adsorption sites may contribute to improve the iodine adsorption capacity.

In this work, 1,2,4,5-tetrakis-(4-formylphenyl)benzene (TPB-CHO) and 2,3,5,6-tetramethyl-*p*-phenylenediamine (TMPD)

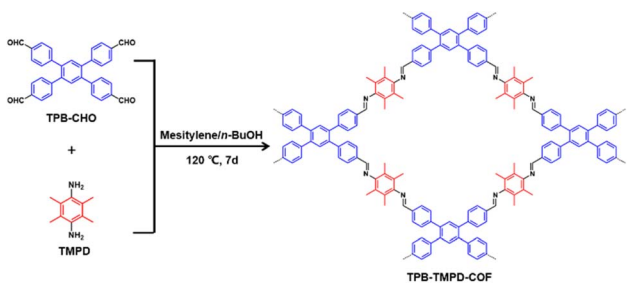


Fig. 1 Synthesis of TPB-TMPD-COF.

*School of Chemical Engineering, Nanjing University of Science and Technology, Nanjing 210094, China. E-mail: hubc@njust.edu.cn*

† Electronic supplementary information (ESI) available. See DOI: https://doi.org/10.1039/d3ra07781k

‡ These authors contributed equally to this work.

were selected to construct a two dimensional COF, named TPB-TMPD-COF, for iodine capture (Fig. 1). TPB-TMPD-COF was well characterized by several techniques and showed long order structure and high surface area. In addition, adsorption experiments showed that the iodine adsorption capacity of TPB-TMPD-COF was 4.75 g $g^{-1}$ under 350 K and normal pressure conditions.

## Results and discussion

The synthetic route of TPB-TMPD-COF is shown in Fig. 1. After condensation of TPB-CHO and TMPD in a mixture of *n*-butanol (1.5 mL), mesitylene (3.5 mL) and 6 M acetic acid aqueous solution (0.6 mL) at 120 °C for 7 days, TPB-TMPD-COF was generated as yellow-green powder in 73% yield, which was insoluble in common solvents. The linkage of TPB-TMPD-COF was confirmed by Fourier transform infrared (FT-IR) spectrum and solid-state $^{13}$C NMR spectra. The FT-IR spectrum of TPB-TMPD-COF displayed a stretching vibration band at ~1636 $cm^{-1}$ (Fig. 2a), confirming the successful formation of imine bonds. And from the $^{13}$C NMR spectroscopy, the characteristic signal appeared at ~160 ppm for TPB-TMPD-COF, indicating the existence of imine bonds again. In addition, the morphology of TPB-TMPD-COF was checked by scanning electron microscopy (SEM), which afforded a prismatic-like morphology (Fig. 2c and d).

The crystallinity of TPB-TMPD-COF was investigated by the powder X-ray diffraction (PXRD) analysis. The PXRD pattern of TPB-TMPD-COF showed strong peaks at 5.0° and 6.3°, and other weak peaks at 9.2°, 9.8°, 12.6°, 13.1°, indicating a high crystallinity. The detailed crystal structure of TPB-TMPD-COF was determined by comparing the experimental PXRD with the simulated PXRD pattern generated by the Accelrys Material Studio software package. In principle, the [4 + 2] connection type may produce four possible crystal structures, single-pore COF with eclipsed (AA) stacking, single-pore COF with staggered (AB) stacking, dual-pore COF with eclipsed (AA) stacking and dual-pore COF with staggered (AB), which were constructed for the structural simulations (Fig. S3 and S4†). It was found that the experimental PXRD pattern of TPB-TMPD-COF could match with simulated PXRD profile of single-pore COF with AA-stacking mode (Fig. S5†). After Pawley refinement, the simulated profile from AA-stacking single-pore mode showed good agreement with the experimental one (Fig. 3a). Finally, the optimized cell parameters of $a = 4.1747$ Å, $b = 19.4152$ Å, $c = 20.0465$ Å, $\alpha = 122.5978°$, $\gamma = 63.9059°$, $\beta = 132.6397°$ with $R_p = 5.01\%$ and $R_{wp} = 7.17\%$ (see Table S1† for details) were obtained.

The permanent porosity of TPB-TMPD-COF was investigated through using nitrogen sorption isotherm recorded at 77 K. Before the measurement, TPB-TMPD-COF had been vacuumed at 80 °C for 12 h. As shown in Fig. 4a, TPB-TMPD-COF displayed the typical type I sorption curve with a sharp uptake at a low relative pressure, which was a significant feature of microporous structure. The Brunauer–Emmett–Teller (BET) model was applied to the isotherm of TPB-TMPD-COF to give a BET surface area of 1090 $m^2$ $g^{-1}$. The total pore volume calculated at $P/P_0 = 0.99$ is 0.49 $cm^3$ $g^{-1}$ for TPB-TMPD-COF. The pore-size distribution of TPB-TMPD-COF exhibited a major peak at 1.5 nm (Fig. 4b), which matched well with the predicted pore size from the simulated crystal structure. The thermal stability of TPB-TMPD-COF was checked by thermogravimetric analysis (Fig. 4c), which showed a high thermal stability up to 400 °C under nitrogen atmosphere. Furthermore, TPB-TMPD-COF was chemically stable in various solvents ($H_2O$, acetone, DMF, hexane) for 24 h (Fig. 4d).

As a potential solid-phase adsorbent for iodine vapor, the capacity of TPB-TMPD-COF was investigated by exposing to iodine vapor at 350 K under normal pressure (Fig. S6†). And before the measurement, the blank control experiment was conducted carefully, which revealed the weight change of the open small vial had little effect on the amount of iodine vapor sorption (Fig. S7†). As shown in Fig. 5a, TPB-TMPD-COF showed a high adsorption capacity with iodine uptake of 4.75 g $g^{-1}$, which was higher than lots of porous materials reported (Table S2†). In addition, thermogravimetric analysis was used to figure

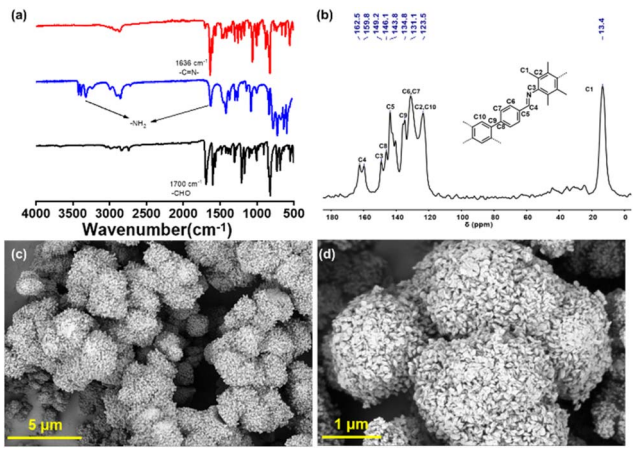


Fig. 2 Synthesis of TPB-TMPD-COF. (a) FT-IR spectra of TPB-CHO (black), TMPD (blue), and TPB-TMPD-COF (red); (b) $^{13}$C NMR spectra of TPB-TMPD-COF; (c and d) SEM image of TPB-TMPD-COF.

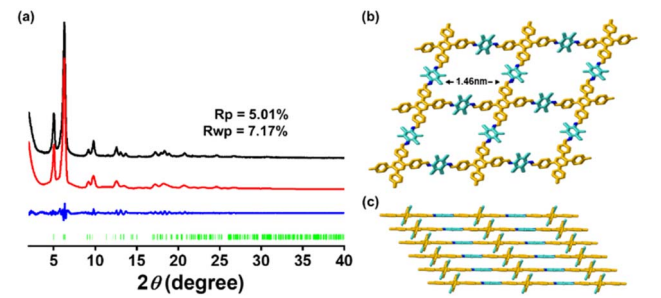


Fig. 3 The experimental and Pawley refined PXRD patterns of TPB-TMPD-COF (a): experimental (black curve), Pawley refined (red curve), difference between the experimental and refined patterns (blue curve), and Bragg position from AA stacking with single-pore structure (green curve). Top view and side view of simulated structure for TPB-TMPD-COF (b and c).

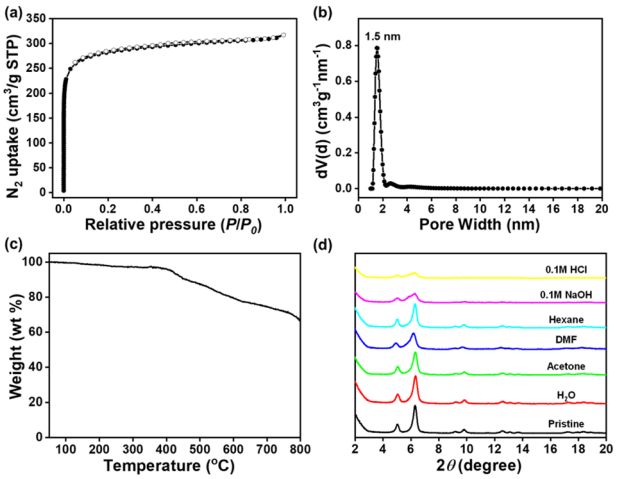


Fig. 4 $N_2$ adsorption–desorption isotherm (a) and pore size distribution (b) of TPB-TMPD-COF; (c) thermogravimetric analysis of TPB-TMPD-COF; (d) PXRD patterns of TPB-TMPD-COF after treatment in different solvents for 24 hours.

out the loss of mass in TPB-TMPD-COF after iodine adsorption (Fig. 5b), which exhibited a significant loss of mass before 300 °C, indicating the escape of iodine species. The observed weight loss was estimated to be 78.8% for TPB-TMPD-COF, comparable to the uptake capacities calculated by gravimetric method. In addition, iodine loaded TPB-TMPD-COF could preserve most of weight upon exposure to air under ambient condition for 5 days (Fig. S8†). Although the surface area and pore volume of TPB-TMPD-COF was lower than that of reported TFPPy-TMPD-COF,[19] the comparable iodine adsorption capacity of TPB-TMPD-COF suggested increasing the density of adsorption sites was an efficient way to improve iodine adsorption capacity.

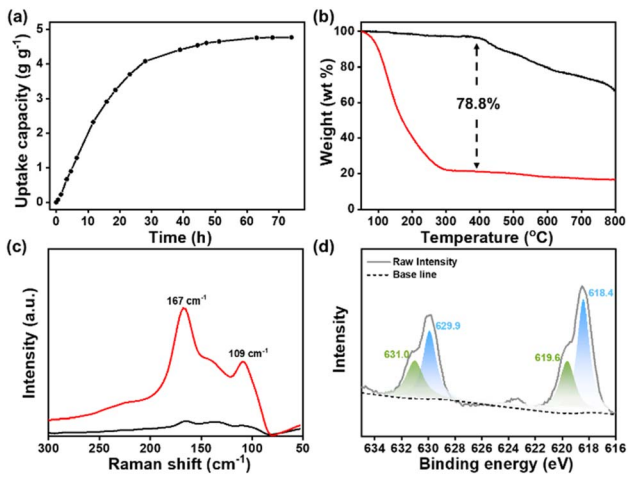


Fig. 5 (a) Uptake of iodine of TPB-TMPD-COF as a function of exposure time at 350 K and ambient pressure; (b) thermogravimetric analysis of TPB-TMPD-COF before (black curve) and after (red curve) iodine uptake; (c) Raman spectra of TPB-TMPD-COF before (black curve) and after (red curve) iodine uptake; (d) XPS I 3d for TPB-TMPD-COF after iodine uptake.

To understand the mechanism of iodine vapor sorption on TPB-TMPD-COF, a series of FT-IR spectroscopy, Raman spectroscopy, X-ray photoelectron spectroscopy (XPS) were performed. As shown in Fig. S9,† a significant shift of the C=N stretching vibration band from 1636 $cm^{-1}$ for TPB-TMPD-COF to 1628 $cm^{-1}$ for iodine loaded TPB-TMPD-COF on FT-IR spectra was observed. Such a shift suggested the strong interaction between the C=N groups and the absorbed iodine molecules, indicating the formation of the charge-transfer species.[22] After uptake of iodine, the Raman spectra of iodine loaded TPB-TMPD-COF presented two characteristic peaks around 109 and 167 $cm^{-1}$ (Fig. 5c), corresponding to $I_3^-$ and $I_5^-$ ions, respectively. The N 1s XPS spectrum of TPB-TMPD-COF displayed a sole peak at 398.8 eV owing to the existence of imine nitrogen atoms (Fig. S10†). After the capture of iodine, a new peak at 400.1 eV was attributed to the formation of N–I bond, confirming the formation of charge-transfer complex between imine bond and iodine again. In addition, two conspicuous peaks located at 629.9 eV and 618.4 eV were observed for iodine loaded TPB-TMPD-COF in I 3d XPS spectral (Fig. 5d), ascribed to I $3d_{3/2}$ and I $3d_{5/2}$ orbitals of polyiodine anions (like $I_3^-$ and $I_5^-$), which was consistent with that obtained from Raman analysis. Furthermore, another two peaks appeared at 631.0 eV and 619.6 eV, corresponding to I $3d_{3/2}$ and I $3d_{5/2}$ orbitals of $I_2$ molecules. The above results exhibited that the iodine vapor adsorbed into the pores may readily generate the electron transfer species ($I_3^-$ and $I_5^-$) due to the strong interactions between imine groups and iodine molecules, indicating a chemisorption step. And then Iodine vapor entered the porous channel through physisorption. In addition, the SEM images showed the morphology of TPB-TMPD-COF was preserved after iodine uptake (Fig. S12†).

Recyclability of TPB-TMPD-COF as adsorbents in iodine vapor capture was also investigated through cycling experiments. After uptake of iodine, TPB-TMPD-COF was regenerated by washing with methanol and drying under vacuum at 120 °C overnight. As shown in Fig. S13,† TPB-TMPD-COF displayed an iodine uptake capacity of 2.8 g $g^{-1}$ after three cycles. FT-IR and PXRD were checked for the regenerated TPB-TMPD-COF (Fig. S14 and S15†), The FT-IR spectrum showed their chemical structure integrity, while their PXRD peak intensities were greatly attenuated, indicating crystallinity decrease significantly. As the ordered structure was very important in iodine uptake, which enabled the full access of the porous space to iodine, the decrease in iodine adsorption capacity of TPB-TMPD-COF may be caused by the crystallinity decrease, which was similar with previous report.[21]

## Conclusions

In summary, a TPB-based 2D COF two-dimensional COF (TPB-TMPD-COF) with specific adsorption of iodine has been successfully synthesized through solvothermal synthesis. TPB-TMPD-COF showed a good crystallinity and a large surface area (1090 $m^2$ $g^{-1}$). More importantly, TPB-TMPD-COF exhibited a vapor iodine capacity of 4.75 g $g^{-1}$ under 350 K and atmospheric pressure conditions, higher than most porous

materials reported. The high adsorption capacity was benefited by the formation of polyiodine anions and the existence of physisorption and chemisorption in the channel of TPB-TMPD-COF. We hope this work will stimulate the design and synthesis of COFs as a solid-phase adsorbent for iodine uptake.

## Author contributions

C. G. performed the synthesis and the characterizations including NMR, PXRD, gas absorption, X. Guan performed the uptake of iodine. Others assisted with the experiments. B. H. supervised the project. C. G. analyzed the data and wrote the paper.

## Conflicts of interest

There are no conflicts to declare.

## Acknowledgements

We gratefully acknowledge financial support from the National Natural Science Foundation of China (22205109, 21975128, 11972178 and 21903044), the Fundamental Research Funds for the Central Universities (30922010812), the Natural Science Foundation of Jiangsu Province (BK20210356).

## References

1 (*a*) R. C. Ewing and F. N. V. Hippel, *Science*, 2009, **325**, 151; (*b*) J. Veliscek-Carolan, *J. Hazard. Mater.*, 2016, **318**, 266.

2 (*a*) K. Xiao, H. Liu, Y. Li, G. Yang, Y. Wang and H. Yao, *Chem. Eng. J.*, 2020, **382**, 122997; (*b*) J. Li, B. Li, N. Shen, L. Chen, Q. Guo, L. Chen, L. He, X. Dai, Z. Chai and S. Wang, *ACS Cent. Sci.*, 2021, **7**, 1441; (*c*) S. U. Nandanwar, K. Coldsnow, V. Utgikar, P. Sabharwall and D. E. Aston, *Chem. Eng. J.*, 2016, **306**, 369; (*d*) B. Li, X. Dong, H. Wang, D. Ma, K. Tan, S. Jensen, B. J. Deibert, J. Bulter, J. Cure, Z. Shi, T. Thonhauser, Y. J. Chabal, Y. Han and J. Li, *Nat. Commun.*, 2017, **8**, 485.

3 (*a*) J. F. Kurisingal, H. Yun and C. S. Hong, *J. Hazard. Mater.*, 2016, **318**, 266; (*b*) Y. Zhong, Y. Mao, S. Shi, M. Wan, C. Ma, S. Wang, C. Chen, D. Zhao and N. Zhang, *ACS Appl. Mater. Interfaces*, 2019, **11**, 32251; (*c*) Y. Mao, Q. Wang, L. Yu, H. Qian, S. Deng, W. Xiao, D. Zhao and C. Chen, *Inorg. Chem.*, 2020, **59**, 8213.

4 (*a*) K.-Y. Geng, T. He, R.-Y. Liu, S. Dalapati, K. T. Tan, Z.-P. Li, S.-S. Tao, Y.-F. Gong, Q.-H. Jiang and D.-L. Jiang, *Chem. Rev.*, 2020, **120**, 8814; (*b*) S. J. Lyle, P. J. Waller and O. M. Yaghi, *Trends Chem.*, 2019, **1**, 172; (*c*) M. S. Lohse and T. Bein, *Adv. Funct. Mater.*, 2018, 1705553; (*d*) Y. Jin, Y. Hu and W. Zhang, *Nat. Rev. Chem*, 2017, **1**, 0056; (*e*) S. Y. Ding and W. Wang, *Chem. Soc. Rev.*, 2013, **42**, 548.

5 A. P. Côté, A. I. Benin, N. W. Ockwig, M. O'Keeffe, A. J. Matzger and O. M. Yaghi, *Science*, 2005, **310**, 1166.

6 (*a*) S. V. Parmar, N. Kumar, M. N. Shewale and V. Avasare, *ChemPhysChem*, 2023, e2022008; (*b*) X.-H. Xiong, L. Zhang, W. Wang, N.-X. Zhu, L.-Z. Qin, H.-F. Huang, L.-L. Meng, Y.-Y. Xiong, M. Barboiu, D. Fenske, P. Hu and Z.-W. Wei, *ACS Appl. Mater. Interfaces*, 2022, **14**, 32105; (*c*) H. Fan, A. Mundstock, A. Feldhoff, A. Knebel, J. Gu, H. Meng and J. Caro, *J. Am. Chem. Soc.*, 2018, **140**, 10094; (*d*) L. Jiang, Y. Tian, T. Sun, Y. Zhu, H. Ren, X. Zou, Y. Ma, K. R. Meihaus, J. R. Long and G. Zhu, *J. Am. Chem. Soc.*, 2018, **140**, 15724; (*e*) S. Zhuo, X. Wang, L. Li, S. Yang and Y. Ji, *ACS Appl. Mater. Interfaces*, 2021, **13**, 31059.

7 (*a*) H. Bhambri, S. Khullar and S. K. Mandal, *Adv. Mater.*, 2022, **3**, 19; (*b*) Z. Li, K. Geng, T. He, K. T. Tan, N. Huang, Q. H. Jiang, Y. K. Nagao and D. Jiang, *Angew. Chem., Int. Ed.*, 2021, **60**, 19419; (*c*) Y. Xiong, Q. Liao, Z. Huang, X. Huang, C. Ke, H. Zhu, C. Dong, H. Wang, K. Xi, P. Zhan, F. Xu and Y. Lu, *Adv. Mater.*, 2020, **32**, e1907242; (*d*) P. Wang, F. Zhou, C. Zhang, S. Y. Yin, L. Teng, L. Chen, X. X. Hu, H. W. Liu, X. Yin and X. B. Zhang, *Chem. Sci.*, 2018, **9**, 8402; (*e*) G. Das, B. P. Biswal, S. Kandambeth, V. Venkatesh, G. Kaur, M. Addicoat, T. Heine, S. Verma and R. Banerjee, *Chem. Sci.*, 2015, **6**, 3931.

8 (*a*) S. H. Hou, W. T. Ji, J. J. Chen, Y. F. Teng, L. P. Wen and L. Jiang, *Angew. Chem., Int. Ed.*, 2021, **60**, 9925–9930; (*b*) X. Zhao, P. Pachfule and A. Thomas, *Chem. Soc. Rev.*, 2021, **50**, 6871–6913; (*c*) J. Lv, Y. X. Tan, J. Xie, R. Yang, M. Yu, S. Sun, M. D. Li, D. Yuan and Y. Wang, *Angew. Chem., Int. Ed.*, 2018, **57**, 12716–12720; (*d*) S. Wang, Q. Wang, P. Shao, Y. Han, X. Gao, L. Ma, S. Yuan, X. Ma, J. Zhou, X. Feng and B. Wang, *J. Am. Chem. Soc.*, 2017, **139**, 4258–4261; (*e*) S. B. Alahakoon, C. M. Thompson, G. Occhialini and R. A. Smaldone, *ChemSusChem*, 2017, **10**, 2116–2129; (*f*) Y. Du, H. Yang, J. M. Whiteley, S. Wan, Y. Jin, S. H. Lee and W. Zhang, *Angew. Chem., Int. Ed.*, 2016, **55**, 1737–1741.

9 (*a*) M. Lu, M. Zhang, J. Liu, Y. F. Chen, J. P. Liao, M. Y. Yang, Y. P. Cai, S. L. Li and Y. Q. Lan, *Angew. Chem., Int. Ed.*, 2022, **61**, e202200; (*b*) A. Jati, K. Dey, M. Nurhuda, M. A. Addicoat, R. Banerjee and B. Maji, *J. Am. Chem. Soc.*, 2022, **144**, 7822; (*c*) Y. Zhao, Y. Zhao, J. Qiu, Z. Li, H. Wang and J. Wang, *ACS Sustain. Chem. Eng.*, 2020, **8**, 18413; (*d*) R. Chen, J.-L. Shi, Y. Ma, G. Lin, X. Lang and C. Wang, *Angew. Chem., Int. Ed.*, 2019, **58**, 6430; (*e*) P. F. Wei, M. Z. Qi, Z. P. Wang, S. Y. Ding, W. Yu, Q. Liu, L. K. Wang, H. Z. Wang, W. K. An and W. Wang, *J. Am. Chem. Soc.*, 2018, **140**, 4623; (*f*) Z. Lu, H. Yang, X. Fu, Y. Zhao, L. Xiao, Z. Zhang and L. Hou, *Macromol. Rapid Commun.*, 2021, **42**, 2100384.

10 P. Wang, Q. Xu, Z. Li, W. Jiang, Q. Jiang and D. Jiang, *Adv. Mater.*, 2018, **30**, 1801991.

11 Y. Xie, T. Pan, Q. Lei, C. Chen, X. Dong, Y. Yuan, J. Shen, Y. Cai, C. Zhou, I. Pinnau and Y. Han, *Angew. Chem., Int. Ed.*, 2021, **60**, 22432.

12 L. He, L. Chen, X. Dong, S. Zhang, M. Zhang, X. Dai, X. Liu, P. Lin, K. Li, C. Chen, T. Pan, F. Ma, J. Chen, M. Yuan, Y. Zhang, L. Chen, R. Zhou, Y. Han, Z. Chai and S. Wang, *Chem*, 2021, **7**, 699.

13 M. Zhou, Z. Li, A. Munyentwali, C. Li, H. Shui and H. Li, *Chem. – Asian J.*, 2022, **17**, e202200358.

14 H. Li, D. Zhang, K. Cheng, Z. Li and P.-Z. Li, *ACS Appl. Nano Mater.*, 2023, **6**, 1295.

15 L. Zhang, J. Li, H. Zhang, Y. Liu, Y. Cui, F. Jin, K. Wang, G. Liu, Y. Zhao and Y. Zeng, *Chem. Commun.*, 2021, **57**, 5558.
16 J. Chang, H. Li, J. Zhao, X. Guan, C. Li, G. Yu, V. Valtchev, Y. Yan, S. Qiu and Q. Fang, *Chem. Sci.*, 2021, **12**, 8452.
17 Y. Zhang, W. Shi, Y. Zhao, C. Zhang and Y. Zhi, *Macromol. Rapid Commun.*, 2023, 2200787.
18 Y. Zhang, Y. Zhi, Y. Zhao, C. Zhang and X. Luo, *CrystEngComm*, 2023, **25**, 525.
19 C. Gao, X. Guan, M. Zhang, H. Hu, L. Chen, C. Sun, C. Zhang, Y. Du and B. Hu, *Macromol. Rapid Commun.*, 2023, 2300311.
20 L. Yang, Y. He, N. Yang, H. Liu and X. Zhu, *Sep. Purif. Technol.*, 2024, **328**, 125054.
21 J. Li, H. Zhang, L. Zhang, K. Wang, Z. Wang, G. Liu, Y. Zhao and Y. Zeng, *J. Mater. Chem. A*, 2020, **8**, 9523.
22 D. Luo, Y. He, J. Tian, J. L. Sessler and X. Chi, *J. Am. Chem. Soc.*, 2022, **144**, 113–117.